RESEARCH ARTICLE

Editorial Process: Submission:11/01/2026 Acceptance:17/08/2026 Published:21/08/2026

Diagnostic Yield and Cost of Morphology-Guided Immunohistochemistry in Liver Tumors

Cheep Charoenlap[1], Pakorn Arunsawat[1], Tanaporn Prateepchaiboon[2], Kittiphan Chienwichai[3], Arunchai Chang[4]*

Abstract

Background: In many routine pathology settings, particularly where resources are constrained, liver tumors are evaluated with an individualized, morphology-guided immunohistochemistry (IHC) strategy rather than fixed panels or molecular assays. Despite widespread use, the real-world diagnostic yield, stain utilization, and laboratory cost of this approach are not well defined. **Methods**: We retrospectively reviewed consecutive malignant liver tumor diagnoses at a university-affiliated hospital from January 2020 to December 2023. Cases were classified as primary liver cancers or metastatic tumors. IHC was performed using a morphology-guided, case-based sequence. Primary outcomes were histologic subtype assignment among primary liver cancers and determination of the primary site among liver metastases. Secondary outcomes were IHC stain utilization and laboratory cost per case. **Results:** Among 279 malignant liver tumors, 144 (51.6%) were primary and 135 (48.4%) were metastatic. Hepatocellular carcinoma accounted for 80.6% of primary liver cancers. Among metastases, a likely primary site was identified in most cases; colorectal (31.1%), lung (9.6%), and pancreatic (8.1%) primaries were most common, while cancers of unknown primary comprised 14.8%. IHC utilization was lower in primary tumors than in metastases (median 2 stains/case [IQR 2–4] vs 4 stains/case [IQR 2–7]; p<0.001). Correspondingly, median laboratory IHC cost per case was lower for primary tumors than for metastases (USD 29.90 [IQR 21.73–51.00] vs USD 46.92 [IQR 21.73–92.57]; p<0.001). **Conclusions:** An individualized, morphology-guided IHC strategy enabled reliable subtyping of primary liver cancers and identification of likely primary sites for most liver metastases while maintaining compact stain utilization and moderate laboratory costs. These data provide practical, real-world benchmarks for diagnostic performance and resource use and support targeted, hypothesis-driven IHC where broad fixed panels or molecular diagnostics are not routinely available.

Keywords: Liver tumors, Immunohistochemistry, Morphology-guided diagnosis, Liver metastases

Asian Pac J Cancer Prev, **27 (8)**, 3081-3088

Introduction

Accurate pathologic classification of liver tumors is essential for clinical decision-making. For primary liver malignancies, particularly hepatocellular carcinoma (HCC) and intrahepatic cholangiocarcinoma (iCCA), histologic subtyping informs eligibility for liver-directed therapies, systemic treatment selection, and prognosis [1-4]. For metastatic tumors involving the liver, determination of the site of origin guides staging, oncologic management, and multidisciplinary planning. In routine practice, these diagnostic objectives rely on the integration of histomorphology with immunohistochemistry (IHC) [5].

In many laboratories, especially in resource-constrained or publicly funded health systems, comprehensive fixed IHC panels and molecular assays are not routinely available. Instead, diagnostic workflows commonly employ a morphology-guided IHC strategy, in which the initial histologic impression directs a limited, hypothesis-driven selection of immunostains. For epithelial tumors, this often involves cytokeratin patterning (e.g., CK7/CK20) followed by targeted lineage- or site-specific markers to confirm hepatocellular differentiation or to support a likely primary site in metastatic disease [4-10]. Although this approach is widely practiced and considered pragmatic, its real-world diagnostic performance and resource utilization have been inadequately quantified.

Existing literature on IHC in liver tumors has largely focused on the diagnostic accuracy of individual markers or predefined panels, frequently in highly selected cohorts or tertiary referral settings [4-10]. Far fewer studies have examined how IHC is actually used in everyday diagnostic

*[1]Department of Anatomical Pathology, Hatyai Hospital, Songkhla, Thailand. [2]Division of Medical Oncology, Department of Internal Medicine, Hatyai Hospital, Songkhla, Thailand. [3]Division of Nephrology, Department of Internal Medicine, Hatyai Hospital, Songkhla, Thailand. [4]Division of Gastroenterology, Department of Internal Medicine, Hatyai Hospital, Songkhla, Thailand. *For Correspondence: busmdcu58@gmail.com*

workflows, particularly with respect to the number of stains required per case, the distribution of stain utilization across tumor types, and the associated laboratory costs [5]. These metrics are increasingly relevant as pathology services face rising test volumes, budgetary constraints, and pressure to optimize tissue utilization without compromising diagnostic confidence.

Diagnostic uncertainty remains common in liver pathology. Poorly differentiated carcinomas, limited biopsy material, overlapping morphologic features, and incomplete clinicoradiologic information can complicate lineage assignment and contribute to cancers of unknown primary (CUP). In these contexts, morphology-guided immunohistochemistry should be interpreted alongside clinicoradiologic findings, especially in resource-limited settings and in tumors with overlapping or deceptive morphologic features, as immunophenotypic results alone may be insufficient for definitive lineage or site assignment. Moreover, empiric expansion of IHC panels may increase costs and tissue consumption without guaranteeing diagnostic resolution [8, 11]. Clear benchmarks describing typical stain utilization, cost per case, and achievable rates of diagnostic classification under a morphology-guided strategy are therefore needed to inform laboratory practice and resource planning.

In this context, we conducted a retrospective study of consecutive malignant liver tumor diagnoses at a university-affiliated hospital in southern Thailand. Using a morphology-guided IHC workflow reflective of routine practice, we aimed to quantify (i) the diagnostic yield of histologic subtype assignment among primary liver cancers, (ii) the rate of primary-site determination among liver metastases, and (iii) immunohistochemistry utilization and laboratory cost per case. By anchoring analysis to stain counts and cost distributions rather than test accuracy alone, this study provides pragmatic benchmarks for laboratories operating without routine access to broad fixed panels or molecular diagnostics.

Materials and Methods

Study design and setting

A retrospective observational study was conducted at a university-affiliated government hospital in southern Thailand. Consecutive liver tissue specimens with a diagnosis of malignancy between 1 January 2020 and 31 December 2023 were reviewed. The study was designed to describe diagnostic classification, immunohistochemistry (IHC) utilization, and laboratory cost in routine practice and followed the STROBE reporting guideline for observational studies.

Case selection and definitions

Eligible cases included the first histopathologic diagnosis of a malignant liver tumor at our institution during the study period. Exclusion criteria were: age <16 years, inadequate tissue for diagnostic interpretation, duplicate specimens from the same diagnostic episode (e.g., re-biopsy or recut), and hematolymphoid malignancies, which were analyzed descriptively but excluded from primary-versus-metastatic epithelial carcinoma comparisons.

Cases were classified into two broad categories

• Primary liver cancers, including hepatocellular carcinoma (HCC), intrahepatic cholangiocarcinoma (iCCA), combined hepatocellular-cholangiocarcinoma, malignant hepatocellular neoplasm not otherwise specified (HCN-NOS), and other rare primary hepatic malignancies, according to the WHO Classification of Digestive System Tumours and Paediatric Tumours, 5th edition [4, 12].

• Metastatic tumors to the liver, classified through integrated assessment of histomorphology, targeted immunohistochemistry, and available clinicoradiologic information rather than on immunohistochemical findings alone. For adenocarcinomas with overlapping morphologic and immunophenotypic features, particularly in the differential diagnosis of iCCA versus metastatic pancreatobiliary or upper gastrointestinal adenocarcinoma, final classification was based on integrated pathologic and clinicoradiologic assessment rather than on immunohistochemistry alone. For metastatic upper gastrointestinal and pancreatobiliary adenocarcinomas, immunohistochemistry was generally used to support or exclude candidate primary sites rather than to establish a site-specific diagnosis in isolation; final attribution reflected multidisciplinary integration of morphologic findings with available imaging, clinical history, and prior pathologic information when available.

Cancer of unknown primary (CUP) was defined as a metastatic liver tumor in which the most likely primary site could not be determined at the time of pathology sign-out despite targeted immunohistochemistry and review of available clinical and imaging data.

Specimen handling and histopathologic review

Specimens included core needle biopsies, wedge biopsies, and surgical resections and were processed according to standard institutional protocols. Hematoxylin- and eosin-stained slides were reviewed by attending pathologists. Cases with diagnostic uncertainty were discussed at departmental consensus conferences prior to final sign-out. For analytic purposes, core needle biopsies and wedge biopsies were combined into a single biopsy category because wedge biopsy cases were few.

Immunohistochemistry strategy

Immunohistochemistry was performed using a morphology-guided, case-based approach rather than fixed diagnostic panels. Initial histologic assessment determined the selection and sequence of immunostains. In diagnostically challenging cases, immunostain selection and interpretation were performed in conjunction with available clinicoradiologic information rather than on immunophenotypic findings alone. Panel selection was not uniform across all specimens; rather, the number and type of immunostains were individualized according to specimen size and adequacy, histomorphologic pattern, and the degree of diagnostic confidence on hematoxylin-eosin sections. In larger specimens or resection samples with classic morphology, diagnosis could often be rendered with limited confirmatory immunostaining or, in

selected cases, without additional immunohistochemistry, whereas small biopsies and poorly differentiated tumors typically required broader targeted workup.

For epithelial tumors, adenocarcinomas were commonly triaged using cytokeratin expression patterns (e.g., CK7 and/or CK20), followed by targeted site- or lineage-specific markers as indicated by morphologic features and available clinical context. The same immunohistochemical panel was not applied uniformly across all adenocarcinoma scenarios; instead, marker selection was tailored to the morphologic pattern, specimen context, and available clinicoradiologic information, including whether the lesion was suspected to represent a primary liver tumor, metastasis from a known extrahepatic primary, or metastasis from an unknown primary. This approach was particularly important in tumors with overlapping morphologic features or potential mimickers, in which immunohistochemistry functioned as a hypothesis-driven adjunct to morphology and clinicoradiologic correlation.

Markers used in routine practice included, but were not limited to, hepatocellular markers (e.g., HepPar-1, Arginase-1, Glypican-3), intestinal markers (e.g., CDX2), pulmonary markers (e.g., TTF-1, Napsin A), renal or gynecologic markers (e.g., PAX8), breast or urothelial markers (e.g., GATA3, estrogen and progesterone receptors), and neuroendocrine markers (e.g., INSM1, chromogranin A, synaptophysin). Neuroendocrine neoplasms were confirmed using a dedicated neuroendocrine marker panel. Marker selection was determined by the attending pathologist and reflected routine diagnostic practice during the study period [4-10, 13, 14]. For clarity, ancillary histochemical stains, if performed in selected cases as part of routine diagnostic workup, were not classified as immunohistochemistry and were not included in the IHC stain-count or cost analyses.

Immunohistochemistry utilization was quantified as the number of distinct antibody-based stains performed per case, with each antibody counted once, regardless of repetition on additional sections.

A schematic summary of the morphology-guided, case-based immunohistochemical workflow used in this study is provided in Figure 1. Representative morphology-based triage categories and photomicrographs of hematoxylin-eosin morphology and corresponding immunohistochemical stains from selected diagnostic scenarios are summarized in Supplementary Table S1.

Outcomes

The primary outcomes of the study were the diagnostic yield of morphology-guided immunohistochemistry, assessed by successful histologic subtype assignment among primary liver cancers, and the determination of the most likely primary site among metastatic liver tumors. Metastatic cases in which a primary site could not be resolved at the time of pathology sign-out despite targeted immunohistochemistry and review of available clinicoradiologic information were classified as CUP.

Secondary outcomes focused on resource utilization, including the number of immunohistochemistry stains performed per case and the laboratory cost per case attributable to immunohistochemistry.

Cost assessment

Unit prices for individual immunohistochemistry stains were obtained from the institutional hospital fee schedule and treated as constant at 2023 price levels. The per-case IHC cost was calculated as the sum of the unit prices of all stains performed for that case. Costs are reported in U.S. dollars (USD, 2023). This analysis was designed to describe laboratory utilization and cost and does not constitute a cost-effectiveness evaluation.

Statistical analysis

Baseline characteristics are summarized as counts (percentages) or mean ± standard deviation, as appropriate. Proportions are presented with percentage. Immunohistochemistry stain counts and costs are reported as median with interquartile range (IQR) because distributions were skewed.

Comparisons of stain utilization and laboratory cost between primary and metastatic tumors were performed

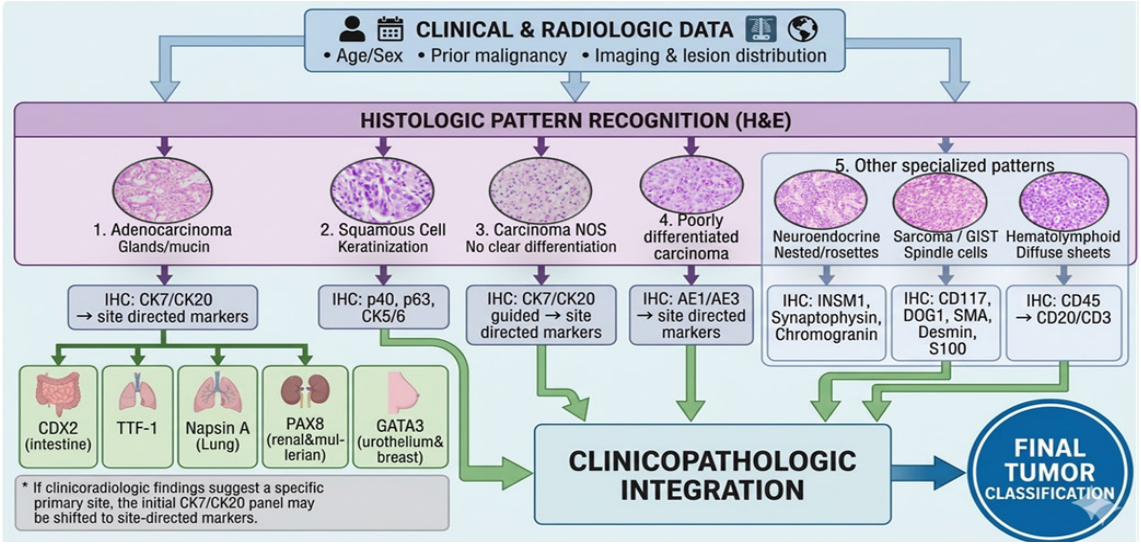

Figure 1. Morphology-Guided Immunohistochemical Workflow for Metastatic Tumors

Table 1. Baseline Characteristics of Patients with Malignant Liver Tumors, Overall and by Tumor Category and Specimen Type

Characteristic	Overall cohort (N = 279)	Primary liver cancers (N = 144)	Metastatic tumors (N = 135)
Overall cohort			
Age, years, mean ± SD	58.8 ± 11.9	59.6 ± 11.0	57.9 ± 12.7
Female sex, n (%)	102 (36.6)	37 (25.7)	65 (48.1)
Male sex, n (%)	177 (63.4)	107 (74.3)	70 (51.9)
Biopsy specimens			
Number of cases, n	210	115	95
Age, years, mean ± SD	58.5 ± 12.0	59.2 ± 11.3	57.6 ± 12.8
Female sex, n (%)	75 (35.7)	30 (26.1)	45 (47.4)
Male sex, n (%)	135 (64.3)	85 (73.9)	50 (52.6)
Resection specimens			
Number of cases, n	69	29	40
Age, years, mean ± SD	59.7 ± 11.6	61.0 ± 10.8	58.8 ± 12.1
Female sex, n (%)	27 (39.1)	7 (24.1)	20 (50.0)
Male sex, n (%)	42 (60.9)	22 (75.9)	20 (50.0)

Footnotes: Values are presented as mean ± standard deviation (SD) or number (percentage), as appropriate.

using the Wilcoxon rank-sum test. Specimen-stratified descriptive analyses were also performed for biopsy and resection specimens. All statistical tests were two-sided, with a significance threshold of $p < 0.05$. Analyses were conducted using R (R Foundation for Statistical Computing).

Ethics

The study protocol was approved by the Institutional Review Board of Hatyai Hospital (Protocol No. HYH EC 051-68-01). Informed consent was waived due to the retrospective design and use of de-identified data.

Results

Cohort characteristics

A total of 279 malignant liver tumors were identified during the study period. Of these, 144 cases (51.6%) were classified as primary liver cancers and 135 cases (48.4%) as metastatic tumors. The overall mean age was 58.8 ± 11.9 years, and 102 patients (36.6%) were female. Female patients were less common among primary liver cancers than among metastatic tumors (25.7% vs. 48.1%).

Biopsy specimens accounted for 210 cases, including 115 primary liver cancers and 95 metastatic tumors, whereas resection specimens accounted for 69 cases, including 29 primary liver cancers and 40 metastatic tumors. The demographic distribution was broadly similar across specimen types, although female patients remained less frequent in the primary liver cancer group than in the metastatic tumor group in both biopsy and resection specimens. Baseline characteristics according to tumor category and specimen type are summarized in Table 1.

Diagnostic classification of primary liver cancers

Among the 144 primary liver cancers, morphology-guided immunohistochemistry enabled classification into standard histologic subtypes in all cases. Hepatocellular carcinoma was the most frequent diagnosis (116/144, 80.6%), followed by intrahepatic cholangiocarcinoma (24/144, 16.7%). Less common entities included combined hepatocellular-cholangiocarcinoma (2/144, 1.4%), malignant hepatocellular neoplasm not otherwise specified (1/144, 0.7%), and primary hepatic angiosarcoma (1/144, 0.7%). Among primary liver cancers, 115 cases were diagnosed on biopsy specimens and 29 on resection specimens. The distribution of histologic subtypes according to specimen type is shown in Table 2.

Primary-site determination among liver metastases

Among the 135 metastatic liver tumors, a likely primary site was identified in the majority of cases using

Table 2. Histologic Subtypes of Primary Liver Cancers According to Specimen Type (N = 144)

Histologic subtype	Total, n (%)	Biopsy, n	Resection, n
Hepatocellular carcinoma	116 (80.6)	92	24
Intrahepatic cholangiocarcinoma	24 (16.7)	19	5
Combined hepatocellular-cholangiocarcinoma	2 (1.4)	2	0
Malignant hepatocellular neoplasm, NOS (HCN-NOS)	1 (0.7)	1	0
Primary hepatic angiosarcoma	1 (0.7)	1	0
Total	144 (100.0)	115	29

Tumors were classified according to the WHO Classification of Digestive System Tumours and Paediatric Tumours, 5th edition; Values are presented as numbers (%); Percentages may not total 100% due to rounding; Biopsy specimens included core needle biopsies and wedge biopsies.

morphology-guided immunohistochemistry integrated with available clinical and imaging information. The most frequent sites of origin were the large intestine (colon and cecum) (42/135, 31.1%), lung (13/135, 9.6%), and pancreas (11/135, 8.1%). Cancer of unknown primary (CUP) accounted for 20 cases (14.8%), representing metastatic tumors in which a primary site could not be determined at the time of pathology sign-out despite targeted immunohistochemistry and review of available clinicoradiologic information. Among metastatic tumors, 95 cases were diagnosed on biopsy specimens and 40 on resection specimens. The full distribution of metastatic primary sites according to specimen type is presented in Table 3.

Table 3. Primary Sites of Origin among Metastatic Liver Tumors According to Specimen Type (N = 135)

Primary site of origin	Total, n (%)	Biopsy, n	Resection, n
Large intestine (colon and cecum)	42 (31.1)	22	20
Lung	13 (9.6)	10	3
Pancreas	11 (8.1)	9	2
Breast	9 (6.7)	6	3
Hematologic malignancy	8 (5.9)	7	1
Stomach	6 (4.4)	4	2
Small intestine (duodenum/jejunum)	4 (3.0)	3	1
Gallbladder	4 (3.0)	3	1
Urinary bladder	4 (3.0)	3	1
Periampullary region	3 (2.2)	2	1
Uterine cervix	2 (1.5)	2	0
Kidney	2 (1.5)	2	0
Ovary	2 (1.5)	2	0
Ampulla of Vater	1 (0.7)	1	0
Esophagus	1 (0.7)	1	0
Nasopharynx	1 (0.7)	1	0
Pharynx	1 (0.7)	1	0
Thymus	1 (0.7)	1	0
Cancer of unknown primary (CUP)	20 (14.8)	15	5
Total	135 (100.0)	95	40

Cancer of unknown primary (CUP) was defined as a metastatic liver tumor in which the most likely primary site could not be determined at the time of pathology sign-out despite targeted immunohistochemistry and review of available clinicoradiologic information. Values are presented as numbers (%). Percentages may not total 100% due to rounding. Biopsy specimens included core needle biopsies and wedge biopsies.

Immunohistochemistry utilization and laboratory cost

Immunohistochemistry utilization differed substantially between primary and metastatic liver tumors. In the overall cohort, primary liver cancers required fewer stains per case than metastatic tumors, with a median of 2 stains (IQR 2–4) versus 4 stains (IQR 2–7), respectively ($p < 0.001$). Correspondingly, the median laboratory cost attributable to immunohistochemistry was lower in primary liver cancers than in metastatic tumors (USD 29.90 [IQR 21.73–51.00] vs. USD 46.92 [IQR 21.73–92.57], $p < 0.001$).

When stratified by specimen type, the difference remained pronounced in biopsy specimens. Primary liver cancers diagnosed on biopsy required a median of 3 stains per case (IQR 2–4), compared with 5.5 stains (IQR 4–8) for metastatic tumors ($p < 0.001$). Median immunohistochemistry cost in biopsy specimens was likewise lower for primary liver cancers than for metastatic tumors (USD 37.10 [IQR 27.30–46.60] vs. USD 65.40 [IQR 39.90–96.60], $p < 0.001$).

In resection specimens, immunohistochemistry utilization was low in both groups, particularly among primary liver cancers. The median number of stains per case was 0 (IQR 0–0) for primary liver cancers and 2 (IQR 0–3) for metastatic tumors ($p = 0.103$). Median

Table 4. Immunohistochemistry Utilization and Laboratory Cost Per Case in Primary versus Metastatic Liver Tumors, Overall and According to Specimen Type

Outcome	Primary liver cancers	Metastatic tumors	p-value*
Overall cohort			
Number of cases, n	144	135	—
Immunohistochemistry stains per case, median (IQR)	2 (2–4)	4 (2–7)	<0.001
Immunohistochemistry cost per case, USD (2023), median (IQR)	29.90 (21.73–51.00)	46.92 (21.73–92.57)	<0.001
Biopsy specimens			
Number of cases, n	115	95	—
Immunohistochemistry stains per case, median (IQR)	3 (2–4)	5.5 (4–8)	<0.001
Immunohistochemistry cost per case, USD (2023), median (IQR)	37.1 (27.3–46.6)	65.4 (39.9–96.6)	<0.001
Resection specimens			
Number of cases, n	29	40	—
Immunohistochemistry stains per case, median (IQR)	0 (0–0)	2 (0–3)	0.103
Immunohistochemistry cost per case, USD (2023), median (IQR)	0 (0–23.3)	19.8 (0–29.0)	0.172

Values are presented as median with interquartile range (IQR), unless otherwise specified; Between-group comparisons were performed using the Wilcoxon rank-sum test because distributions were skewed; Costs represent laboratory charges calculated using 2023 unit prices and are reported in U.S. dollars (USD); This analysis describes immunohistochemistry utilization and laboratory cost and does not constitute a cost-effectiveness evaluation; Biopsy specimens included core needle biopsies and wedge biopsies; Interpretation of findings in resection specimens is limited by the small number of cases and should therefore be approached with caution.

immunohistochemistry cost per case was USD 0.00 (IQR 0.00–23.30) for primary liver cancers and USD 19.80 (IQR 0.00–29.00) for metastatic tumors (p = 0.172). These findings are summarized in Table 4.

Morphologic patterns and supplementary analyses

Supplementary analyses further describe the morphology-guided diagnostic framework and stain utilization across tumor subtypes. A summary of the morphology-based triage categories and representative confirmatory immunohistochemical markers used in this study is provided in Supplementary Table S1. The distribution of morphologic categories among metastatic liver tumors is shown in Supplementary Table S2. Immunohistochemistry utilization, laboratory cost, and key marker usage by primary liver cancer subtype are presented in Supplementary Table S3, whereas corresponding analyses by metastatic histologic pattern, including the rate of cancer of unknown primary, are shown in Supplementary Table S4.

Discussion

This four-year retrospective study demonstrates that a morphology-guided immunohistochemistry (IHC) strategy provides reliable diagnostic classification of liver tumors in routine practice while maintaining relatively compact stain utilization and laboratory costs. Using a workflow reflective of everyday diagnostic decision-making, primary liver cancers were consistently subtyped, and a likely site of origin was identified for the majority of liver metastases. Importantly, the number of stains and associated costs were substantially lower for primary liver cancers than for metastatic tumors, underscoring the efficiency of hypothesis-driven IHC selection guided by histomorphology. This contrast was most evident in biopsy specimens, whereas immunohistochemistry utilization was low overall in resection specimens, particularly among primary liver cancers.

Several findings merit emphasis. First, the high rate of successful histologic classification among primary liver cancers highlights the diagnostic value of combining classic morphologic features with a limited set of hepatocellular markers. In this cohort, hepatocellular carcinoma accounted for more than four-fifths of primary liver malignancies, and confirmation typically required few immunostains. This pattern reflects the fact that many primary hepatic tumors retain characteristic architectural and cytologic features that narrow the differential diagnosis early, allowing targeted confirmation rather than broad immunophenotypic screening. The relatively low stain utilization observed in primary tumors, therefore, represents an expected and desirable outcome of morphology-guided practice rather than under-investigation. This lower stain utilization likely also reflects differences in specimen context, as larger or morphologically classic specimens may permit confident diagnosis with limited ancillary confirmation, whereas small biopsies more often require broader targeted immunohistochemical evaluation. The specimen-stratified results support this interpretation, as primary liver cancers diagnosed on resection specimens showed minimal immunohistochemical use, whereas biopsy specimens more often required confirmatory staining.

Second, the distribution of primary sites among metastatic liver tumors aligns with established epidemiologic patterns, with colorectal, lung, and pancreatic primaries predominating [2, 9]. Nevertheless, metastatic tumors required more extensive immunohistochemical workup, reflected by higher median stain counts and laboratory costs. This increase is clinically intuitive: metastatic lesions often lack organ-specific architectural cues, particularly in poorly differentiated carcinomas, necessitating broader lineage and site-directed testing. This is particularly relevant for upper gastrointestinal and pancreatobiliary adenocarcinomas, in which CK7/CK20 profiles and markers such as CDX2 are often overlapping and non-definitive; in these cases, immunohistochemistry functioned mainly as a supportive and exclusionary tool, whereas final site attribution depended on multidisciplinary integration rather than on IHC alone. Even within a morphology-guided framework, diagnostic resolution in this setting inherently demands greater resource use than in primary hepatic neoplasia [5-9]. This difference was especially apparent in biopsy specimens, in which metastatic tumors required substantially more stains and incurred higher laboratory costs than primary liver cancers, whereas comparisons in resection specimens were more limited and should be interpreted cautiously given the smaller subgroup size.

Despite targeted immunohistochemistry, a subset of metastatic tumors remained classified as cancer of unknown primary. The observed CUP rate reflects real-world diagnostic constraints rather than failure of the IHC strategy itself. Limited biopsy material, overlapping immunophenotypes, and incomplete clinicoradiologic information at the time of sign-out all contribute to unresolved primary-site assignment. An important conceptual limitation is that intrahepatic cholangiocarcinoma and metastatic pancreatobiliary or upper gastrointestinal adenocarcinomas may show substantial morphologic and immunophenotypic overlap; accordingly, site assignment in these cases should be understood as a multidisciplinary interpretation integrating pathology with available clinical and imaging findings rather than as an IHC-only determination. In contrast to studies from high-resource centers that incorporate extensive fixed panels or routine molecular profiling, the present study reflects practice in settings where escalation options are finite. Within this context, the CUP rate provides a realistic benchmark for diagnostic yield achievable using morphology-guided IHC alone [7, 15]. Importantly, this rate should be interpreted as a sign-out-level diagnostic endpoint rather than a definitive final clinical diagnosis, because downstream radiologic, endoscopic, pathologic, or molecular investigations after sign-out were not systematically captured and may have reclassified some cases.

From a resource-utilization perspective, the contrast between primary and metastatic tumors is particularly informative. The finding that median laboratory costs nearly doubled for metastatic cases underscores how tumor

biology and diagnostic uncertainty directly influence resource consumption. Importantly, these data should be interpreted as a cost and utilization description, not as a cost-effectiveness analysis. No inferences are made regarding downstream clinical outcomes or comparative economic value of alternative diagnostic strategies. Instead, the results offer practical reference points for laboratories seeking to balance diagnostic thoroughness with cost containment. The specimen-specific analyses further suggest that biopsy specimens represent the setting in which morphology-guided stain selection may have the greatest practical impact on resource utilization.

Comparison with prior literature further contextualizes these findings. Previous studies evaluating IHC use in liver metastases, including reports from tertiary referral centers, have similarly emphasized the effectiveness of case-based, morphology-driven approaches in limiting unnecessary staining. However, most prior work has focused on stain counts or diagnostic concordance without incorporating cost data [5]. By integrating stain utilization with laboratory cost per case, the present study extends existing knowledge and provides metrics that are directly relevant to laboratory management and health system planning.

This study has several strengths. The use of consecutive cases over multiple years minimizes selection bias and captures routine diagnostic behavior rather than idealized workflows. Reporting of proportions and use of medians for skewed distributions enhances interpretability. The addition of specimen-stratified analyses further improves the practical interpretability of the findings by showing how immunohistochemistry utilization differed between biopsy and resection specimens. Inclusion of a morphology-based triage framework in the supplementary material further improves transparency and reproducibility without implying rigid diagnostic algorithms. The proposed schematic workflow is intended to illustrate the pragmatic morphology-guided triage strategy used in routine practice rather than to prescribe a fixed universal algorithm, because final panel selection remained dependent on morphologic interpretation, specimen context, and clinicoradiologic correlation.

Several limitations should be acknowledged. The retrospective, single-center design may limit generalizability to institutions with different case mixes, marker availability, or reimbursement structures. In addition, morphology-guided immunohistochemistry is inherently vulnerable to tumors with morphologic overlap or potential mimickers, particularly when tissue is limited or clinicoradiologic information is incomplete. In such cases, immunostains are best interpreted as a hypothesis-driven adjunct to morphology and clinicoradiologic correlation, rather than as an isolated determinant of diagnosis. Furthermore, because immunohistochemical panel selection in routine practice was individualized by the attending pathologist, differences in pathologist experience, morphologic interpretation, and availability of clinical or radiologic information may have introduced case-level and temporal variation in stain selection, which could have influenced both diagnostic yield and laboratory cost. Misclassification of metastatic origin therefore remains possible in selected cases. Molecular assays and broad next-generation sequencing were not incorporated and therefore could not be evaluated as escalation strategies for unresolved cases. This limitation is especially relevant in resource-limited settings, where broad fixed panels and molecular escalation may not be routinely available. In addition, although specimen-stratified analyses were performed, some resection-based subgroups remained small and the corresponding comparisons should be interpreted cautiously. Finally, operational outcomes such as turnaround time and tissue exhaustion were not assessed and warrant future study.

In summary, this study provides real-world benchmarks for diagnostic yield, immunohistochemistry utilization, and laboratory cost in the evaluation of liver tumors using a morphology-guided approach. The findings support the continued role of histomorphology as the foundation of diagnostic decision-making and illustrate how targeted immunohistochemistry can achieve clinically meaningful classification without routine reliance on large fixed panels. The revised specimen-specific analyses further show that these differences are most apparent in biopsy specimens, where diagnostic uncertainty is typically greatest and judicious stain selection is most consequential. These data may inform laboratory policy, resource allocation, and future prospective evaluations of stepwise diagnostic pathways in liver pathology.

Author Contribution Statement

Conceptualization: C.C., A.C.; Methodology: C.C., P.A.; K.C., A.C.; Data Curation: C.C., P.A., T.P., K.C.; Writing—Original Draft Preparation: C.C., A.C.; Writing—Review and Editing: C.C., A.C.; Supervision: A.C. All authors had full access to the data, contributed to data interpretation, approved the final manuscript, and agree to be accountable for all aspects of the work..

Acknowledgements

The authors thank the pathology laboratory staff at Hatyai hospital for their support with slide preparation and immunostaining, and the multidisciplinary hepatobiliary team for clinical collaboration. We are grateful to administrative team for assistance with data management.

Consent for publication

Not applicable; the dataset was de-identified prior to analysis and contains no individual person's data in any form.

Ethics approval and consent to participate

This retrospective study was approved by the Institutional Review Board of Hatyai Hospital (Protocol No. HYH EC 051-68-01; approval date 27 May 2025). Given the use of de-identified data and minimal risk, the requirement for informed consent was waived in accordance with institutional policy and the Declaration of Helsinki.

Competing interests

The authors declare no competing interests relevant to this work.

Availability of data and materials

The de-identified dataset and analysis code are available from the corresponding author upon reasonable request. Data sharing is contingent on institutional policies and ethical approvals.

References

1. Ferlay J, Ervik M, Lam F, Laversanne M, Colombet M, Mery L, Piñeros M, et al. Global Cancer Observatory: Cancer Today. Lyon, France: International Agency for Research on Cancer [Internet]. 2024.
2. American Cancer Society. Overview of liver cancer types and frequency of metastases to the liver from other primary cancers [Internet]. Atlanta (GA): American Cancer Society; 2024 [cited 2026 Aug 10]. Available from: https://www.cancer.org/cancer/types/liver-cancer/about/what-is-liver-cancer.html.
3. Rusyn I, Lemon SM. Mechanisms of HCV-induced liver cancer: what did we learn from in vitro and animal studies? Cancer Lett. 2014;345(2):210–5. https://doi.org/10.1016/j.canlet.2013.06.028
4. Paradis V, Fukayama M, Sakamoto M, Park YN. Tumours of the liver and intrahepatic bile ducts. In: WHO Classification of Tumours Editorial Board, editor. Digestive system tumours. 5th ed. Lyon (France): International Agency for Research on Cancer; 2019. p. 229-39.
5. Wang JD, Sebastian C, Walther Z, Suresh T, Lacy J, Zhang X, et al. An appraisal of immunohistochemical stain use in hepatic metastasis highlights the effectiveness of the individualized, case-based approach: analysis of data from a tertiary care medical center. Arch Pathol Lab Med. 2023;147(2):185–92. https://doi.org/10.5858/arpa.2021-0457-OA
6. Selves J, Long-Mira E, Mathieu MC, Rochaix P, Ilié M. Immunohistochemistry for diagnosis of metastatic carcinomas of unknown primary site. Cancers (Basel). 2018;10(4):108. https://doi.org/10.3390/cancers10040108
7. Laprovitera N, Riefolo M, Ambrosini E, Klec C, Pichler M, Ferracin M. Cancer of unknown primary: challenges and progress in clinical management. Cancers (Basel). 2021;13(3):451. https://doi.org/10.3390/cancers13030451
8. Bellizzi AM, Montgomery EA, Hornick JL. American Registry of Pathology expert opinions: evaluation of poorly differentiated malignant neoplasms on limited samples—gastrointestinal mucosal biopsies. Ann Diagn Pathol. 2020;44:151419. https://doi.org/10.1016/j.anndiagpath.2019.151419
9. Amin K, El-Rayes D, Snover D, Mettler T, Vogel RI, Khalifa MA. Patterns of immunohistochemistry utilization in metastases to the liver. Appl Immunohistochem Mol Morphol. 2019;27(6):441–7. https://doi.org/10.1097/PAI.0000000000000643
10. Koehne de Gonzalez AK, Salomao MA, Lagana SM. Current concepts in the immunohistochemical evaluation of liver tumors. World J Hepatol. 2015;7(10):1403–11. https://doi.org/10.4254/wjh.v7.i10.1403
11. Jaber O, Ammar K, Sughayer M. Communicating uncertainty in pathology reports: a descriptive study from a specialized cancer center. Acad Pathol. 2024;11(1):100109. https://doi.org/10.1016/j.acpath.2024.100109.
12. Lam-Tse WK, Chan SJ, Gauthier C, Hsu E, Meyers HR, Ranganathan S, et al. Paediatric hepatocellular carcinoma. In: WHO Classification of Tumours Editorial Board, editor. Paediatric tumours. 5th ed. Lyon (France): International Agency for Research on Cancer; 2022.
13. Liberini V, Huellner MW, Grimaldi S, Finessi M, Thuillier P, Muni A, et al. The challenge of evaluating response to peptide receptor radionuclide therapy in gastroenteropancreatic neuroendocrine tumors: the present and the future. Diagnostics (Basel). 2020;10(12):1083. https://doi.org/10.3390/diagnostics10121083.
14. Rooper LM, Sharma R, Li QK, Illei PB, Westra WH. INSM1 demonstrates superior performance to the individual and combined use of synaptophysin, chromogranin, and CD56 for diagnosing neuroendocrine tumors of the thoracic cavity. Am J Surg Pathol. 2017;41(11):1561–9. https://doi.org/10.1097/PAS.0000000000000916.
15. Lee MS, Sanoff HK. Cancer of unknown primary. BMJ. 2020;371:m4050. https://doi.org/10.1136/bmj.m405.